Title

Inhibitory Interactions between Phosphorylation Sites in the C Terminus of α-Amino-3-hydroxy-5-methyl-4-isoxazolepropionic Acid-type Glutamate Receptor GluA1 Subunits*

Journal

Journal of Biological Chemistry, 289(21)

ISSN

0021-9258

Authors

Gray, Erin E
Guglietta, Ryan
Khakh, Baljit S
et al.

Publication Date

2014-05-01

DOI

10.1074/jbc.m114.553537

Peer reviewed

THE JOURNAL OF BIOLOGICAL CHEMISTRY VOL. 289, NO. 21, pp. 14600–14611, May 23, 2014

Inhibitory Interactions between Phosphorylation Sites in the C Terminus of α-Amino-3-hydroxy-5-methyl-4-isoxazolepropionic Acid-type Glutamate Receptor GluA1 Subunits*

Received for publication, January 28, 2014, and in revised form, March 25, 2014 Published, JBC Papers in Press, April 4, 2014, DOI 10.1074/jbc.M114.553537

Erin E. Gray[‡§], **Ryan Guglietta**[‡§], **Baljit S. Khakh**[‡¶], **and Thomas J. O'Dell**[‡‖1]

From the [‡]*Department of Physiology and* [¶]*Department of Neurobiology, David Geffen School of Medicine at UCLA,* [§]*Interdepartmental Ph.D. Program for Neuroscience at UCLA, and* [‖]*UCLA Integrative Center for Learning and Memory, Los Angeles, California 90095*

Background: AMPA receptor (AMPAR) GluA1 subunits contain multiple phosphorylation sites.
Results: Distinct Ca^{2+}-dependent signaling pathways regulate GluA1 phosphorylation at Thr-840 and Ser-845, and phosphorylation of one site inhibits phosphorylation of the other.
Conclusion: Interactions between Thr-840 and Ser-845 provides a mechanism for conditional regulation of AMPARs.
Significance: Our results reveal a novel mechanism for regulating AMPAR function at excitatory synapses.

The C terminus of AMPA-type glutamate receptor (AMPAR) GluA1 subunits contains several phosphorylation sites that regulate AMPAR activity and trafficking at excitatory synapses. Although many of these sites have been extensively studied, little is known about the signaling mechanisms regulating GluA1 phosphorylation at Thr-840. Here, we report that neuronal depolarization in hippocampal slices induces a calcium and protein phosphatase 1/2A-dependent dephosphorylation of GluA1 at Thr-840 and a nearby site at Ser-845. Despite these similarities, inhibitors of NMDA-type glutamate receptors and protein phosphatase 2B prevented depolarization-induced Ser-845 dephosphorylation but had no effect on Thr-840 dephosphorylation. Instead, depolarization-induced Thr-840 dephosphorylation was prevented by blocking voltage-gated calcium channels, indicating that distinct Ca^{2+} sources converge to regulate GluA1 dephosphorylation at Thr-840 and Ser-845 in separable ways. Results from immunoprecipitation/depletion assays indicate that Thr-840 phosphorylation inhibits protein kinase A (PKA)-mediated increases in Ser-845 phosphorylation. Consistent with this, PKA-mediated increases in AMPAR currents, which are dependent on Ser-845 phosphorylation, were inhibited in HEK-293 cells expressing a Thr-840 phosphomimetic version of GluA1. Conversely, mimicking Ser-845 phosphorylation inhibited protein kinase C phosphorylation of Thr-840 *in vitro*, and PKA activation inhibited Thr-840 phosphorylation in hippocampal slices. Together, the regulation of Thr-840 and Ser-845 phosphorylation by distinct sources of Ca^{2+} influx and the presence of inhibitory interactions between these sites highlight a novel mechanism for conditional regulation of AMPAR phosphorylation and function.

Phosphorylation-dependent changes in the activity and trafficking of postsynaptic α-amino-3-hydroxy-5-methyl-4-isoxazolepropionic acid-type glutamate receptors (AMPARs)[2] are thought to have a key role in NMDA receptor (NMDAR)-dependent forms of synaptic plasticity such as long term potentiation (LTP) and long term depression (LTD) (1, 2). Functional AMPARs are formed from tetrameric combinations of different subunits (GluA1-GluA4), and previous studies have identified a number of phosphorylation sites in the cytoplasmic C-terminal tails of these subunits that may be involved in synaptic plasticity (3). One AMPAR subunit in particular, the GluA1 subunit, contains four phosphorylation sites clustered within a short stretch of 27 amino acids in its C terminus that are especially important in both LTP and LTD. For instance, protein kinase C (PKC) phosphorylation of GluA1 subunits at serine 818 may be involved in the synaptic insertion of AMPARs into excitatory synapses after the induction of LTP (4). In addition, PKC or calcium/calmodulin-dependent kinase II (CaMKII) phosphorylation of GluA1 at serine 831 (5–7) likely contributes to the increase in AMPAR channel conductance that occurs after LTP induction (8–13). Protein kinase A (PKA) phosphorylation of GluA1 subunits at Ser-845 also has an important role in AMPAR trafficking (14, 15) and the enhancement of LTP by modulatory neurotransmitters acting through the cAMP/PKA signaling pathway (16–18). Moreover, dephosphorylation of Ser-845 is thought to contribute to decreases in synaptic strength in LTD (19–22), in part by regulating activity-dependent AMPAR endocytosis (23, 24).

AMPAR GluA1 subunits are also phosphorylated at Thr-840 (25–28). Although Thr-840 dephosphorylation may have a role

* This work was supported, in whole or in part, by National Institutes of Health Grants MH609197 (to T. J. O.) and T32MH85462 and MH91384 (to E. E. G.).
[1] To whom correspondence should be addressed: Dept. of Physiology, David Geffen School of Medicine at UCLA, 53-231 Center for the Health Sciences, Box 951751, Los Angeles, CA 90095-1751. Tel.: 310-206-4654; Fax: 310-206-5661; E-mail: todell@mednet.ucla.edu.

[2] The abbreviations used are: AMPAR, α-amino-3-hydroxy-5-methyl-4-isoxazolepropionic acid-type glutamate receptor; ACSF, artificial cerebrospinal fluid; APV, amino-phosphonovaleric acid; CamKII, calcium/calmodulin-dependent kinase II; fEPSP, field excitatory postsynaptic potential; FSK, forskolin; LTD, long term depression; LTP, long term potentiation; NMDAR, *N*-methyl-D-aspartate receptor; PP1, protein phosphatase 1; PP2A, protein phosphatase 2A; PP2B, protein phosphatase 2B; VGCC, voltage-gated calcium channel.

in LTD (25), little is known about the upstream signaling pathways underlying activity-dependent changes in phosphorylation of this site. Indeed, fundamental questions, such as the effects of Thr-840 phosphorylation on AMPAR function and the protein kinases responsible for Thr-840 phosphorylation *in vivo* are only partly understood.

The close proximity of Thr-840 and Ser-845 in the C terminus of GluA1 is intriguing, as previous studies have shown that clusters of multiple phosphorylation sites can give rise to interactions whereby phosphorylation at one site can enhance or inhibit subsequent phosphorylation of nearby sites (29–32). Although interactions between phosphorylation sites appear to be a common signaling motif in postsynaptic density proteins (32, 33), potential interactions between phosphorylation sites in the C terminus of GluA1 have not yet been investigated. Here, we addressed these questions by examining the mechanisms underlying activity-dependent changes in GluA1 phosphorylation at Thr-840 and Ser-845. Our results indicate that surprisingly distinct calcium-dependent signaling pathways drive GluA1 dephosphorylation at Thr-840 and Ser-845 during neuronal depolarization and suggest that these sites exhibit bidirectional, inhibitory interactions.

MATERIALS AND METHODS

Acute Hippocampal Slice Preparation—Standard methods approved by the University of California, Los Angeles Institutional Animal Care and Use Committee were used to prepare 400-μm-thick hippocampal slices from C57Bl/6 male mice between the ages of 8 and 12 weeks. Animals were deeply anesthetized with isoflurane and sacrificed by cervical dislocation. The brain was rapidly removed and placed into cold (4 °C), oxygenated (95% O_2/5% CO_2) artificial cerebral spinal fluid (ACSF) containing 124 mM NaCl, 4.4 mM KCl, 25 mM Na_2HCO_3, 1 mM NaH_2PO_4, 1.2 mM $MgSO_4$ 2 mM $CaCl_2$, and 10 mM glucose. Techniques described elsewhere (25) were then used to prepare and maintain slices *in vitro* (at 30 °C). Field excitatory postsynaptic potentials (fEPSPs) evoked by Schaffer Collateral fiber stimulation (0.02 Hz) were recorded in stratum radiatum of the CA1 region using ACSF-filled, glass microelectrodes (5–10 megohm resistance). Signals were acquired and analyzed using pClamp 10 (Molecular Devices). Slices were allowed to recover for at least 2 h before an experiment.

Reagents and Antibodies—Forskolin (FSK), chelerythrine, Gö6976 (LC Laboratories), KN-62 (Cayman Chemical), thapsigargin, rolipram, cantharidin, and cyclosporin A (Tocris Bioscience) were prepared as concentrated stock solutions in DMSO. Isoproterenol (Tocris Bioscience) and D-APV (Abcam) were prepared as concentrated stock solutions in H_2O. All other chemicals were obtained from Sigma. Anti-phospho-Thr-840 antibody (1:2000) was from Abcam, whereas total GluA1, phospho-Ser-831, and phospho-Ser-845 antibodies (all used at 1:1000) were from Millipore. Antibodies against β-actin (1:5,000) and a neuronal specific isoform (βIII) of tubulin (1:20,000) were from Sigma. Horseradish peroxidase conjugated secondary antibodies (1:2000) were obtained from GE Healthcare.

Western Immunoblotting—Homogenates from treated and untreated hippocampal slices were prepared using techniques described elsewhere (25). For GluA1-expressing HEK293 cells, pharmacological stimulation with FSK (1 μM) was performed by adding drug directly to medium containing the cells and incubated at 37 °C for 10 min. The cells were then washed briefly in PBS and incubated on ice in homogenization buffer containing Complete Lysis-M Reagent (Roche Applied Science), 25 mM *n*-dodecyl-β-maltoside, Protease Inhibitor Complete (Roche Applied Science), and Phosphatase Inhibitor Cocktails I and II (Sigma). Cells were scraped from the plate and briefly sonicated before being diluted in 2× sample loading buffer and boiled. Proteins were separated by SDS-PAGE (20 μg per lane), and standard procedures were used for Western immunoblotting. For quantification of Westerns using slice homogenates, all values were first normalized to levels of tubulin in each lane to control for variations in loading and then expressed as a percent of untreated control slices. With HEK-293 cells, levels of total GluA1 were normalized to actin for each sample, and this GluA1:actin ratio was then used to correct for variability in recombinant protein expression levels.

Immunoprecipitation with Phospho-specific GluA1 Antibodies—Hippocampal slices maintained *in vitro* were snap-frozen and homogenized in 200 μl of modified radioimmune precipitation assay buffer containing 50 mM Tris, pH 7.4, 150 mM NaCl, 1% Nonidet P-40, 0.5% deoxycholate, 0.1% SDS, 10 mM EGTA, 10 mM EDTA, 25 mM sodium pyrophosphate, 10 μM cantharidin (Tocris Bioscience), phosphatase inhibitor cocktails I and II (Sigma), and Protease Inhibitor Complete (Roche Applied Science). For the input sample, 50 μl (~140 μg) of protein lysate was removed, rocked overnight at 4 °C, and boiled in an equal volume of 2× loading buffer. The immunoprecipitation was performed by incubating 100 μl (~350 μg) of the protein lysate with 4 μg of phospho-Thr-840 or phospho-Ser-845 antibody for 5 h at 4 °C followed by binding to Protein A Plus-agarose beads (Pierce) at 4 °C with rocking overnight. Beads were then pelleted by centrifugation, and half the volume of supernatant was removed (50 μl) and boiled in an equal volume of 2× loading buffer (depleted sample). The beads were washed 3 times in wash buffer (50 mM Tris, pH 7.4, 300 mM NaCl, 5 mM EGTA, 0.1% Triton), resuspended in 1× loading buffer (100 μl), and boiled (immunoprecipitated sample). Equal volumes were loaded for Western blotting.

Phosphopeptide/Antibody Competition Assays—Hippocampal homogenates were prepared using modified radioimmune precipitation assay buffer, and proteins were separated by SDS-PAGE (20 μg per lane). Alternate lanes in each gel (10 total) contained either prestained molecular weight markers (Kaleidoscope, Bio-Rad) or hippocampal samples. After transfer onto nitrocellulose membranes, individual lanes containing hippocampal protein were cut from the blot using the molecular weight markers as a guide and then incubated with either phospho-Ser-845- or phospho-Thr-840-specific antibodies (1:4000 dilution for both) in the absence or presence of different concentrations of phosphorylated peptides corresponding to amino acids 836–850 in the C terminus of GluA1 subunits (New England Peptide). After incubation in primary and secondary antibodies the blot was reassembled, and bands were imaged using enhanced chemiluminescence. Blots were reprobed with anti-tubulin antibodies to control for potential

variations in loading. The concentration of peptide that inhibited antibody recognition of phospho-GluA1 by 50% (IC^{50}) was calculated by fitting the results to the following equation,

$$y = \text{min} + (\text{max-min})/(1 + ([\text{peptide}]/IC_{50})^h) \quad \text{(Eq. 1)}$$

where y = band density normalized to control (no added peptide), [peptide] = concentration of the competing phosphopeptide, and h is the Hill coefficient. Curve fitting was done using SigmaPlot (SPSS, Inc.).

GST Fusion Protein Purification and in Vitro Kinase Assays—The C terminus of GluA1 (814–889) fused to GST (GST-GluA1: the plasmid pGEX-4T-3 GluR1CT was kindly provided by Dr. Soderling, Oregon Health and Science University) was expressed in *Escherichia coli* BL21 cells and affinity-purified with glutathione-Sepharose 4B (GE Healthcare) according to the manufacturer's instructions. Purified CaMKII (New England Biolabs), PKA (New England Biolabs), PKCα (Millipore), or p70S6 kinase (Millipore) were incubated with 6.0 μg of GST-GluA1 in 100-μl reactions using buffer conditions and kinase unit concentrations recommended by the manufacturer. Reactions were incubated for 0–30 min at 30 °C and stopped by the addition of SDS-PAGE loading buffer, and the protein (1 μg per lane) was resolved by SDS-PAGE. Western blotting with phosphospecific antibodies was used to measure phosphorylation. Mutations to GST-GluA1 were introduced at Thr-840 and Ser-845 using the QuikChange Site-directed Mutagenesis kit (Stratagene) and verified by DNA sequencing.

HEK-293 Cell Culture and Electrophysiology—HEK-293 cells were maintained in DMEM supplemented with 10% fetal bovine serum, penicillin, and streptomycin (all from Invitrogen) at 37 °C in a humidified cell culture incubator containing 5% CO_2. Cells were transiently transfected in a 6-well plate at 40–60% confluence using Effectene Reagent (Qiagen) and were used for experiments 48 h later. Wild type or mutant YFP-GluA1 cDNA were used for transfections; the mutations were generated using the QuikChange Site-directed Mutagenesis kit (Stratagene). Before electrophysiological experiments, the cells were gently mechanically dispersed and plated onto poly-L-lysine-coated glass coverslips and maintained at 37 °C for 2–8 h. Immediately before recording, the coverslip was transferred to a recording chamber at 22–23 °C and continually perfused with extracellular recording solution containing 147 mM NaCl, 2 mM KCl, 1 mM $MgCl_2$, 1 mM $CaCl_2$, 10 mM HEPES, and 10 mM glucose (pH = 7.4, ~300 mosM). Glutamate (10 mM, 100 ms) was applied locally through a barrel of a fast perfusion device (SF-77B Perfusion Fast Step, Warner Instruments) every 1–2 min. Solutions containing FSK (50 μM) plus the phosphodiesterase inhibitor rolipram (0.1 μM) or vehicle (0.11% DMSO) were delivered continually for 15 min through a second barrel starting 5 min after break-in. Whole-cell voltage-clamp recordings were performed with borosilicate glass electrodes (5–7 megohms) filled with 140 mM KCl, 4 mM MgATP, 11 mM EGTA, 1 mM $CaCl_2$, 10 mM HEPES, 2 mM tetraethylammonium chloride, and 10 mM phosphocreatine (pH = 7.2, 295 mosM) using an Axopatch 200 amplifier (Molecular Devices). Data were acquired and analyzed using pClamp 8.1/Campfit software (Molecular Devices). Cells were held at −60 mV, and series resistance was continually monitored throughout the experiment. If the holding current was unstable or if the series resistance (typically 10–15 megaohms) changed by >20% during the experiment, the cell was discarded.

Statistics—All results are presented as the mean ± S.E. Statistical significance was determined using paired and unpaired t tests, one-way analysis of variance or, where appropriate, one-way analysis of variance on ranks. Student-Newman-Keuls tests for multiple comparisons were used for post hoc comparisons. One-way repeated measures of analysis of variance followed by Bonferroni t test comparisons to base line were used to determine statistical significance of FSK/rolipram-induced increases in glutamate-evoked currents in HEK-293 cells.

RESULTS

GluA1 Phosphorylation at Thr-840 and Ser-845 Is Regulated by Distinct Ca^{2+} and Protein Phosphatase Signaling Pathways—To examine the activity-dependent regulation of GluA1 phosphorylation at Thr-840, we first measured changes in GluA1 phosphorylation induced by transient neuronal depolarization in hippocampal slices. As shown in Fig. 1*A*, a 5-min bath application of ACSF containing elevated potassium levels (50 mM KCl; hereafter referred to simply as high-K^+) rapidly abolished synaptic transmission in hippocampal slices (due to depolarization block) but had no lasting effect on synaptic transmission (40 min post high-K^+ application fEPSPs were 110 ± 6% of base line, $n = 6$, $p = 0.13$ compared with base line). To examine the effects of depolarization on GluA1 phosphorylation, slices from the same animal were either unstimulated (untreated controls) or exposed to high-K^+ ACSF for 5 min and then collected for analysis immediately after high-K^+ stimulation or at different time points after high-K^+ ACSF washout (15 and 35 min). Depolarization induced by high-K^+ ACSF triggered a significant decrease in GluA1 phosphorylation at Thr-840 (phospho-Thr-840 GluA1 levels were reduced to 56 ± 5% that of untreated control slices, $p < 0.05$ compared with control, $n = 7$) that rapidly recovered after high-K^+ washout (Fig. 1*B*). Depolarization also induced a significant decrease in GluA1 Ser-845 phosphorylation (levels were reduced to 50 ± 4% of untreated controls, $p < 0.05$) (Fig. 1*B*). However, unlike Thr-840, Ser-845 phosphorylation showed little recovery even 40 min after depolarization (Fig. 1*B*). Similarly, direct activation of NMDARs with bath application of ACSF containing 20 μM NMDA for 3 min transiently blocked synaptic transmission but had no lasting effect on synaptic strength (40 min post-NMDA application fEPSPs were 109 ± 5% of base line, $n = 4$) (Fig. 1*C*) and induced a transient dephosphorylation of GluA1 at Thr-840 and a persistent decrease in Ser-845 phosphorylation ($n = 6$) (Fig. 1*D*).

Results from previous studies using either chemical LTD induction protocols or low frequency synaptic stimulation suggest that LTD is associated with persistent GluA1 Ser-845 dephosphorylation (19–21). It was thus surprising that under our experimental conditions both high-K^+ ACSF and NMDA application induced a persistent decrease in GluA1 Ser-845 phosphorylation yet had no lasting effect on synaptic strength. Thus, to examine changes in GluA1 phosphorylation at Thr-840 and Ser-845 associated with LTD, we repeated experiments

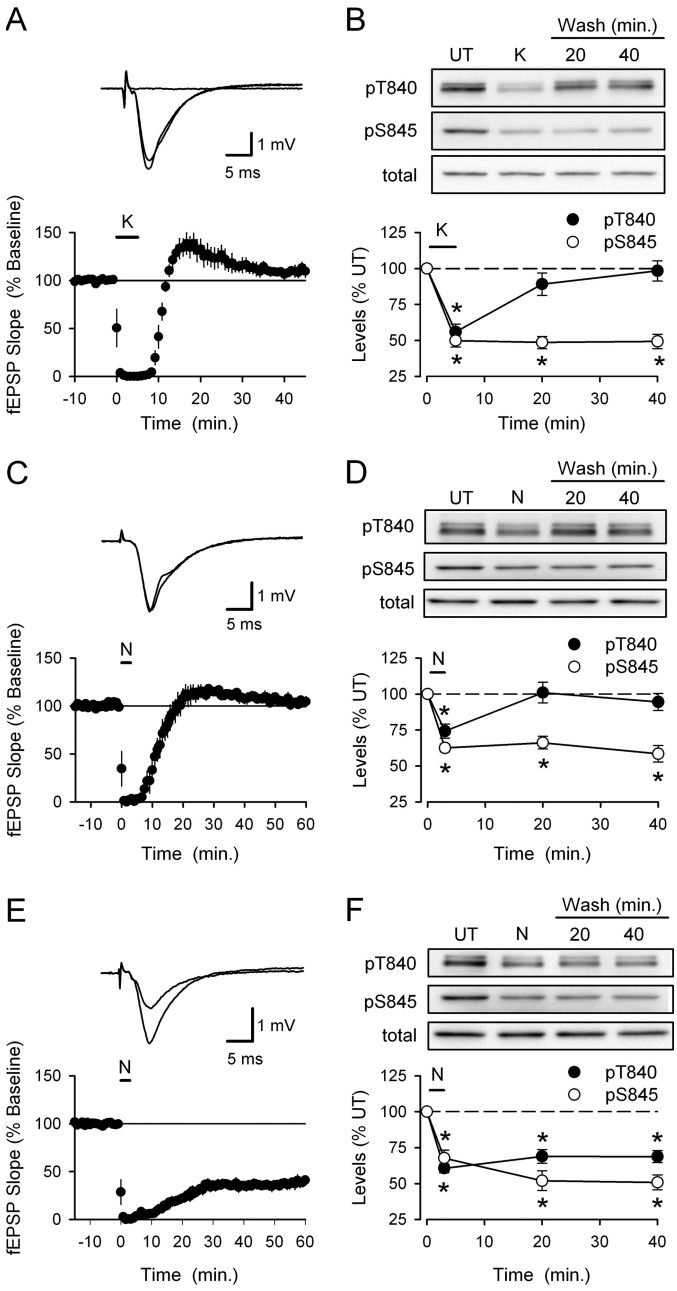

FIGURE 1. **Changes in GluA1 phosphorylation at Thr-840 and Ser-845 induced by transient depolarization and NMDAR activation.** *A*, bath application of high-K^+ ACSF (50 mM, indicated by the *bar*) transiently abolishes transmission but has no lasting effect on synaptic strength ($n = 6$). Traces show example fEPSPs recorded during base line in the presence of high-K^+ ACSF and 40 min after high-K^+ washout. *B*, phospho-Thr-840 (*pT840*) and phospho-Ser-845 (*pS845*) GluA1 levels in hippocampal slices that were either untreated (*UT*) or exposed to a 5-min bath application of high-K^+ ACSF and collected either immediately after high-K^+ application (*K*) or after high-K^+ washout for 15 or 35 min ($n = 8$, $^*p < 0.05$ compared with untreated controls). *C*, bath application of NMDA (20 μM for 3 min, indicated by the *bar*) induces a transient inhibition of synaptic transmission ($n = 4$). Traces show example fEPSPs recorded during base line and 60 min post-NMDA application. *D*, changes in GluA1 Thr-840 and Ser-845 phosphorylation induced by NMDAR activation ($n = 6$; *, $p < 0.05$). *E*, bath application of NMDA (20 μM for 3 min) in high-Ca^{2+} ACSF induces LTD ($n = 7$). Traces show fEPSPs recorded during base line and 60 min after NMDA application. *F*, changes in GluA1 Thr-840 and Ser-845 phosphorylation induced by NMDA application in high-Ca^{2+} ACSF ($n = 7$; *, $p < 0.05$). Total GluA1 levels were not altered by high-K^+ ACSF or application of NMDA application in normal or high-Ca^{2+} ACSF.

using bath application of NMDA in ACSF containing 4.0 mM Ca^{2+} (high-Ca^{2+} ACSF), a protocol that reliably induces LTD in the CA1 region of hippocampal slices from adult animals (25, 34). As shown in Fig. 1*E*, bath application of NMDA (20 μM for 3 min) in high-Ca^{2+} ACSF induced robust LTD (40 min post NMDA application fEPSPs were reduced to 39 ± 5% that of base line, $n = 7$, $p < 0.001$ compared with base line). The persistent dephosphorylation of GluA1 at Ser-845 induced by NMDA application in high-Ca^{2+} ACSF was similar to that seen in slices exposed to NMDA in normal Ca^{2+} ACSF (Fig. 1*F*). However, consistent with previous observations (25), bath application of NMDA in the presence of high-Ca^{2+} ACSF induced a persistent decrease in GluA1 phosphorylation at Thr-840 (Fig. 1*F*). Thus, changes in GluA1 phosphorylation at Thr-840 exhibit a better correlation with changes in synaptic strength.

Consistent with previous findings showing that NMDA-induced Ser-845 dephosphorylation is calcium-dependent (35), high-K^+ induced dephosphorylation of both Thr-840 and Ser-845 was almost completely prevented when high-K^+ was applied in Ca^{2+}-free ACSF containing 10 mM EGTA (Fig. 2, *A* and *B*). In contrast, disrupting calcium release from intracellular stores with thapsigargin (2 or 5 μM, 1 h pretreatment) had no effect on depolarization-induced dephosphorylation of either Thr-840 ($n = 6$) or Ser-845 ($n = 4$), suggesting that calcium release from intracellular stores is not involved (Fig. 2*C*). Thus, depolarization-induced Thr-840 and Ser-845 dephosphorylation is triggered by increases in intracellular calcium due to activation of ligand-gated and/or voltage-gated calcium channels (VGCCs).

Because the changes in GluA1 Thr-840 and Ser-845 phosphorylation induced by high-K^+ are similar to those seen after pharmacological activation of NMDARs (Fig. 1), we examined whether depolarization-induced dephosphorylation of GluA1 at these sites is mediated by NMDAR activation. Blocking NMDARs with D-APV (50 μM) prevented depolarization-induced dephosphorylation of Ser-845 but, surprisingly, had no effect on Thr-840 dephosphorylation (Fig. 2*D*). Blocking L-type VGCCs with nifedipine (50 μM) either alone ($n = 4$) or in the presence of APV ($n = 2$) also had no effect on high-K^+-induced Thr-840 dephosphorylation (data not shown). Depolarization-induced Thr-840 dephosphorylation was, however, strongly inhibited in the presence of 3.0 mM $CoCl_2$, a blocker of multiple types of VGCCs (Fig. 2*D*). Blocking VGCCs with Co^{2+} also prevented depolarization-induced Ser-845 phosphorylation (Fig. 2*D*), most likely by preventing NMDAR activation by blocking depolarization-induced glutamate release from presynaptic terminals. Consistent with this notion, synaptic transmission was abolished in the presence of 3.0 mM $CoCl_2$ (Fig. 2*E*). Together, these results suggest that although increases in intracellular Ca^{2+} trigger GluA1 dephosphorylation at both Thr-840 and Ser-845, Thr-840 dephosphorylation is dependent on activation of VGCCs, whereas NMDAR-mediated increases in intracellular Ca^{2+} regulate Ser-845 phosphorylation.

To determine the protein phosphatases responsible for depolarization-induced GluA1 dephosphorylation at Thr-840 and Ser-845, hippocampal slices from the same animal were exposed to ACSF containing either 0.1–0.2% DMSO (vehicle

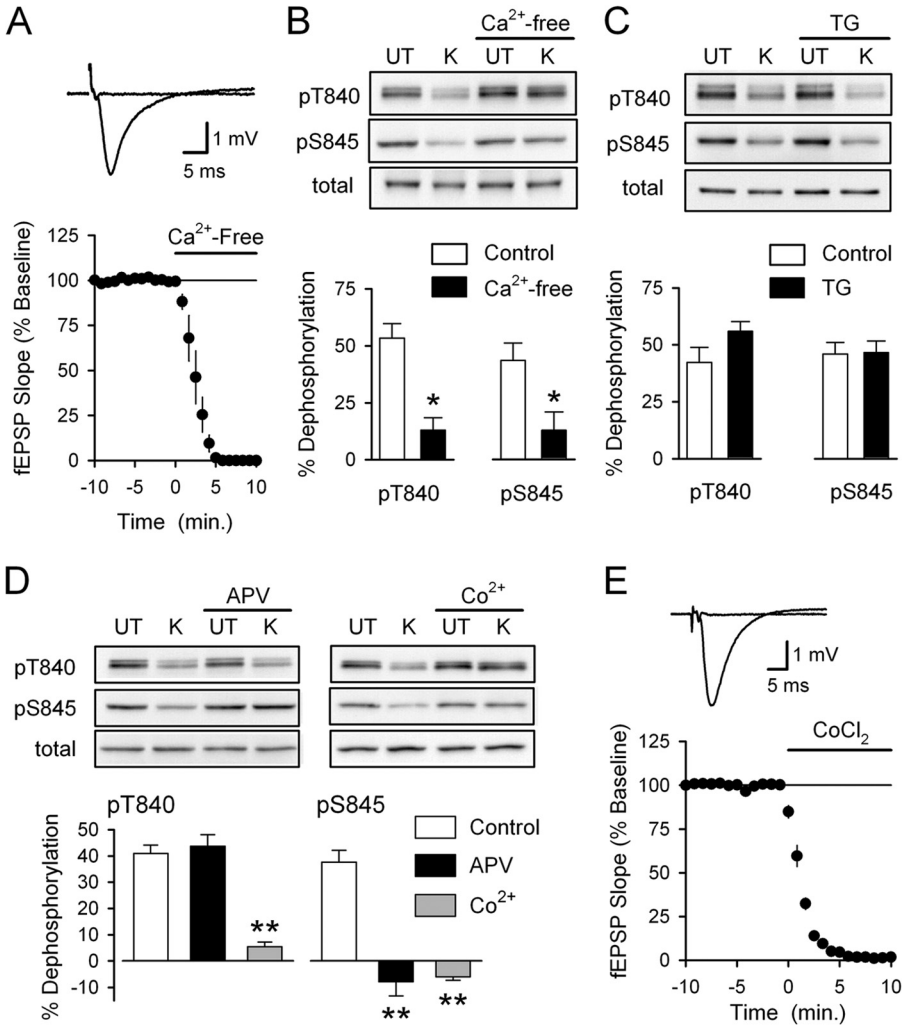

FIGURE 2. **Distinct sources of Ca^{2+} influx are responsible for depolarization-induced Thr-840 and Ser-845 dephosphorylation.** *A*, a 10-min bath application of Ca^{2+}-free ACSF containing 10 mM EGTA (indicated by the *bar*) blocks excitatory synaptic transmission ($n = 4$). Traces show example fEPSPs recorded during base line and after application of Ca^{2+}-free ACSF. *B*, slices were either untreated (*UT*) or exposed to high-K^+ (*K*) ACSF in the absence and presence of 10 mM EGTA (Ca^{2+}-free, 10 min pretreatment) ($n = 5$; *, $p < 0.05$ compared with % dephosphorylation in absence of EGTA). Ca^{2+}-free ACSF had no effect on basal levels of GluA1 Thr-840 (*pT840*) and Ser-845 (*pS845*) phosphorylation or total GluA1 levels. *C*, inhibiting Ca^{2+} release from intracellular stores with thapsigargin (*TG*) had no effect on high-K^+ induced GluA1 dephosphorylation at Thr-840 and Ser-845. Slices were pretreated (for 1 h) with ACSF containing either 0.1% DMSO (vehicle control, $n = 6$) or 2.0–5.0 μM thapsigargin ($n = 4$ and 2, respectively). Thapsigargin had no effect on total GluA1 levels or basal levels of GluA1 phosphorylation at Thr-840 and Ser-845. *D*, high-K^+ was applied in the absence (control, $n = 8$) or presence of either 50 μM D-APV ($n = 5$) or 3 mM $CoCl_2$ ($n = 3$). Although blocking VGCC with Co^{2+} inhibited depolarization-induced dephosphorylation at both Thr-840 and Ser-845, blocking NMDARs with APV only prevented dephosphorylation of GluA1 at Ser-845 (**, $p < 0.001$ compared with % dephosphorylation in controls). APV and $CoCl_2$ had no effect on basal levels of GluA1 phosphorylation at either site, and total GluA1 levels were unchanged in all conditions. *E*, bath application of ACSF containing 3.0 mM $CoCl_2$ abolishes synaptic transmission ($n = 4$). Traces show fEPSPs recorded during base line and 10 min after application of ACSF containing $CoCl_2$.

controls) or different protein phosphatase inhibitors for 1–2 h before high-K^+ induced depolarization. Previous studies have found that inhibitors of protein phosphatase 1 (PP1) and protein phosphatase 2A (PP2A), such as okadaic acid and calyculin A, enhance GluA1 phosphorylation at both Ser-845 and Thr-840 (19, 25, 26, 36). Consistent with these observations, cantharidin, an inhibitor of PP1 and PP2A (37), increased basal levels of GluA1 phosphorylation at Thr-840 and Ser-845 (levels were increased to 196 ± 12 and 214 ± 12% that of vehicle-treated controls, respectively, $p < 0.05$ compared with control, $n = 6$) and inhibited depolarization-induced dephosphorylation of both sites (Fig. 3, *A, C,* and *D*). In contrast, the protein phosphatase 2B (PP2B) inhibitor cyclosporin A (2.0 μM) had no effect on basal levels of GluA1 phosphorylation at Thr-840 and Ser-845 (levels were 87 ± 6 and 102 ± 12% that of vehicle-treated control slices respectively, $n = 8$) and did not inhibit depolarization-induced Thr-840 dephosphorylation (Fig. 3, *B* and *C*). Cyclosporin A did, however, significantly inhibit depolarization-induced Ser-845 dephosphorylation (Fig. 3, *B* and *D*). Thus, the depolarization-induced decrease in GluA1 phosphorylation at Thr-840 and Ser-845 not only involves distinct sources of Ca^{2+} but also arises from activation of distinct, but overlapping, types of protein phosphatases.

Thr-840 Is Phosphorylated by PKC in Vitro and in Hippocampal Slices—Although p70S6 kinase (25) and PKC (26) can both phosphorylate Thr-840 *in vitro*, the identity of the protein kinase(s) responsible for Thr-840 phosphorylation in neurons is unclear. We thus used both *in vitro* and *in vivo* approaches to identify the protein kinases that phosphorylate Thr-840. As shown in Fig. 4*A*, *in vitro* kinase assays using GST fusion pro-

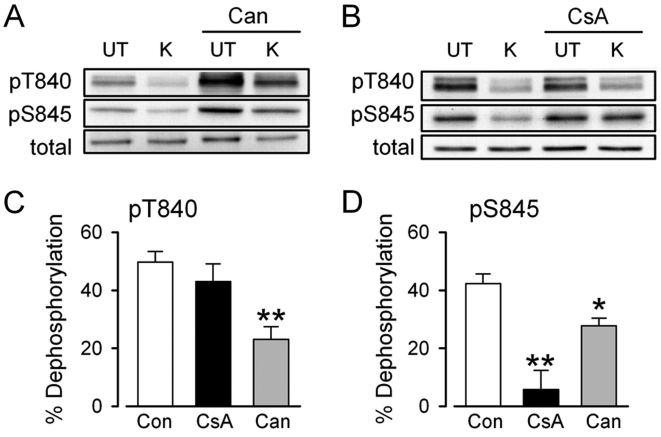

FIGURE 3. **Protein phosphatases mediating depolarization-induced GluA1 dephosphorylation.** *A*, immunoblots showing levels of phospho-Thr-840, phospho-Ser-845, and total GluA1 in an experiment where high-K^+ (*K*) was applied in the presence of ACSF containing 0.1% DMSO (vehicle control) or 20 μM cantharidin (*Can*). *UT*, untreated. *B*, same as in *panel A* but with 2.0 μM cyclosporin A (*CsA*) pretreatment. *C* and *D*, summary of changes in GluA1 phosphorylation at Thr-840 (*pT840*; *C*) and Ser-845 (*pS845*; *D*) induced by high-K^+ ACSF in control slices ($n = 14$) and in slices where high-K^+ ACSF was applied in the presence of cantharidin ($n = 6$) or cyclosporin A ($n = 8$). *$p < 0.05$, **$p < 0.001$ compared with % dephosphorylation induced by high-K^+ in vehicle control-treated slices. *Con*, control.

teins containing the C terminus of GluA1 indicate that Thr-840 can be phosphorylated by multiple protein kinases including PKC, p70S6 kinase, and CaMKII. As expected from previous studies (25, 26), PKA did not phosphorylate GluA1 at Thr-840 but readily phosphorylated Ser-845 (Fig. 4*A*). To determine which of these candidate protein kinases phosphorylate Thr-840 in neurons, we examined whether re-phosphorylation of Thr-840 after high-K^+-induced dephosphorylation was inhibited in the presence of different protein kinase inhibitors. Consistent with a previous report that PKC phosphorylates Thr-840 in hippocampal neurons (26), re-phosphorylation of Thr-840 after a 5-min application of high-K^+ ACSF was significantly inhibited in hippocampal slices exposed to ACSF containing the PKC inhibitors Gö6976 (2 μM) or chelerythrine (10 μM) (Fig. 4, *B* and *C*). In contrast, the CaMKII inhibitor KN-62 (10 μM) had no effect on Thr-840 re-phosphorylation (Fig. 4, *B* and *C*). Although this suggests that CaMKII activation does not contribute to Thr-840 phosphorylation after high-K^+-induced depolarization, KN-62 inhibits CaMKII activation but does not inhibit autophosphorylated, persistently active forms of this kinase (38). Thus, these results do not rule out a potential role for CaMKII in Thr-840 phosphorylation *in vitro*.

GluA1 Phosphorylation at Thr-840 Inhibits Ser-845 Phosphorylation—Thr-840 and Ser-845 are phosphorylated by basophilic protein kinases (25, 26, 39, 40) (Fig. 4), which preferentially phosphorylate substrates with positively charged residues in close proximity to the phosphorylation site (41). The close proximity of Thr-840 and Ser-845 in the C terminus of GluA1 thus suggests that the addition of a negatively charged phospho group at one of these sites could alter this preferred recognition sequence and inhibit the ability of protein kinases to phosphorylate the nearby site. To test this hypothesis, we first used an immunoprecipitation/depletion assay to compare PKA-mediated increases in Ser-845 phosphorylation at Thr-840-phosphorylated and non-Thr-840-phosphorylated GluA1.

As shown in Fig. 5*A*, immunoprecipitation with a phospho-Thr-840 GluA1-specific antibody effectively removes Thr-840-phosphorylated GluA1 from lysates prepared from hippocampal slices (phospho-Thr-840 GluA1 levels in the unbound fraction after a single round of immunoprecipitation were just $0.4 \pm 0.2\%$ that of the levels in total lysate, $n = 8$). Thus, immunoprecipitation with anti-phospho-Thr-840 GluA1 antibodies provides a convenient way to separate Thr-840-phosphorylated GluA1 (immunoprecipitated fraction) and non-Thr-840-phosphorylated GluA1, which remains in the supernatant after immunoprecipitation (unbound fraction). Immunoblotting with phospho-Ser-845-specific antibodies can then be used to measure GluA1 Ser-845 phosphorylation in each of these fractions.

Fig. 5*B* shows the results of experiments using this approach. In these experiments hippocampal slices were either untreated or exposed to a 3-min bath application of ACSF containing the β-adrenergic receptor agonist isoproterenol to activate PKA signaling. Phospho-Thr-840 immunoprecipitation was then used to deplete Thr-840-phosphorylated GluA1 from lysates prepared from both groups of slices, and immunoblotting with anti-phospho-Ser-845 GluA1 antibodies was used to measure Ser-845 phosphorylation in the total lysate, the immunoprecipitated fraction (Thr-840-phosphorylated GluA1), and in the unbound fraction (non-Thr-840-phosphorylated GluA1). Consistent with the notion that GluA1 phosphorylation at Thr-840 can inhibit phosphorylation of Ser-845, the isoproterenol-induced increase in Ser-845 phosphorylation was significantly smaller in the immunoprecipitated fraction compared with that seen in both the total lysate ($p < 0.01$) and in the non-Thr-840-phosphorylated GluA1/unbound fraction ($p < 0.05$) (Fig. 5*B*).

Although the results shown in Fig. 5*B* suggest that prior Thr-840 phosphorylation inhibits PKA phosphorylation of GluA1 at Ser-845, a similar result could occur if Thr-840-phosphorylated GluA1 is already highly phosphorylated at Ser-845 in hippocampal slices under basal conditions. To examine this possibility, we used immunoprecipitation/depletion assays with anti-phospho-Ser-845 GluA1 antibodies to determine the basal levels of Ser-845 phosphorylation on Thr-840-phosphorylated GluA1. In these experiments immunoprecipitation with anti-phospho-Ser-845 antibodies effectively cleared Ser-845-phosphorylated GluA1 from lysates prepared from untreated hippocampal slices (levels were depleted to $0.7 \pm 0.2\%$ compared with total lysate, $n = 8$) but reduced levels of Thr-840-phosphorylated GluA1 by only $30 \pm 4\%$ (Fig. 5*A*). This indicates that Thr-840-phosphorylated GluA1 is not also highly phosphorylated at Ser-845. Indeed, this value is most likely an overestimation of the pool of GluA1 subunits phosphorylated at both Thr-840 and Ser-845 as AMPARs in hippocampal neurons are predominately GluA1/GluA2 heterodimers (42) with a subunit stoichiometry of 2:2 (43, 44). Thus the reduction in Thr-840-phosphorylated GluA1 in the unbound fraction after phospho-Ser-845 GluA1 immunoprecipitation represents the removal of receptors where Ser-845 and Thr-840 are phosphorylated on the same subunit as well as receptors where one GluA1 subunit was phosphorylated at Ser-845 and the other GluA1 subunit was phosphorylated at Thr-840.

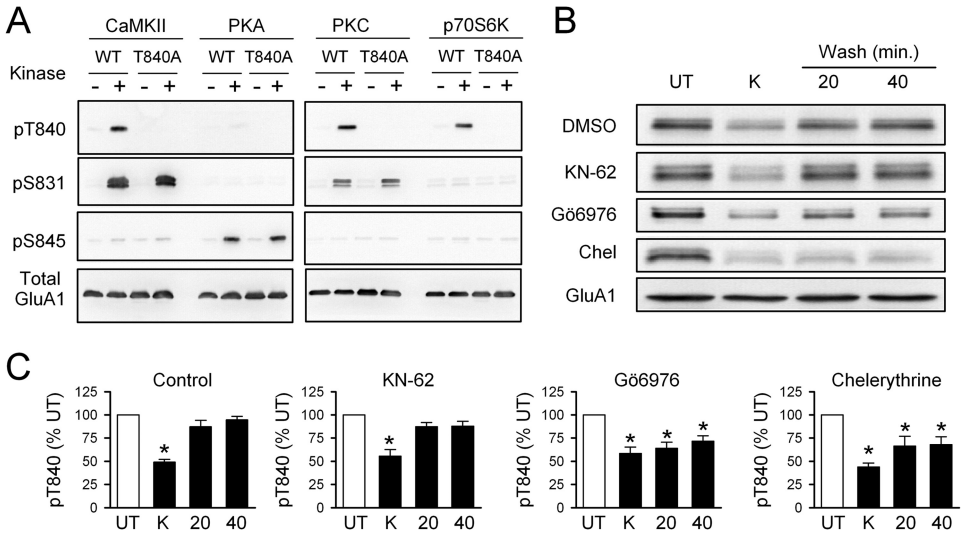

FIGURE 4. **PKC phosphorylates GluA1 at Thr-840 *in vitro* and *in vivo*.** *A*, *in vitro* phosphorylation assay using purified protein kinases and a C-terminal GluA1-GST fusion protein. Thr-840 (*pT840*) is phosphorylated by CaMKII, PKC, and p70S6 kinase. Phosphorylation by all three protein kinases was disrupted when Thr-840 was mutated to an alanine (T840A). *UT*, untreated. *B*, immunoblots show changes in Thr-840 phosphorylation after application of high-K^+ (*K*) ACSF in the continuous presence of different protein kinase inhibitors. *Chel*, chelerythrine. *C*, summary of experiments shown in *B*. Depolarization induced a transient dephosphorylation of AMPAR GluA1 subunits at Thr-840 in vehicle control slices (0.1–0.2% DMSO, $n = 7$) and in slices exposed to 10 μM KN-62 ($n = 4$). Thr-840 re-phosphorylation was significantly inhibited in the presence of 10 μM chelerythrine ($n = 6$) or 2.0 μM Gö6976 ($n = 5$, $^*p < 0.05$ compared with untreated).

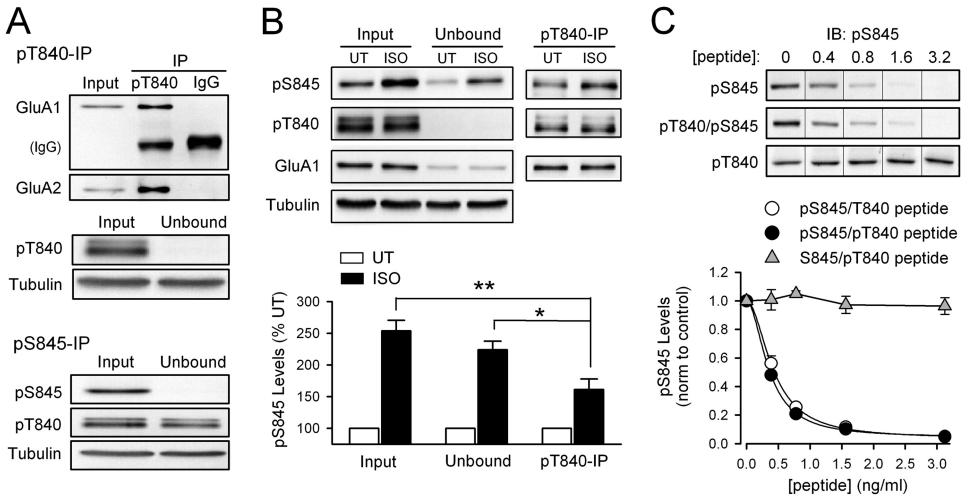

FIGURE 5. **GluA1 Thr-840 phosphorylation inhibits Ser-845 phosphorylation in hippocampal slices.** *A*, homogenates prepared from untreated (*NT*) hippocampal slices were cleared of phospho-Thr-840 (*pT840*; *top*) or phospho-Ser-845 GluA1 (*pS845*; *bottom*) by immunoprecipitation (*IP*) with phospho-specific antibodies ($n = 8$ for each). *IgG*, non-immune IgG control immunoprecipitation. Note co-immunoprecipitation of AMPAR GluA2 subunits (*top*) and the small reduction of Thr-840-phosphorylated GluA1 in the unbound fraction after immunoprecipitation of Ser-845-phosphorylated GluA1 (*bottom*). *UT*, untreated. *B*, PKA activation downstream of β-adrenergic receptor activation preferentially phosphorylates non-Thr-840-phosphorylated GluA1 in hippocampal slices. Anti-phospho-Thr-840 antibodies were used to immunoprecipitate Thr-840-phosphorylated GluA1 (*pT840*) from lysates prepared from untreated (*UT*) control slices and slices exposed to isoproterenol (*ISO*; 1 μM, 3 min) ($n = 4$). The isoproterenol-induced increase in Ser-845 phosphorylation (*pS845*) in Thr-840-phosphorylated (*pT840*) GluA1 (immunoprecipitate fraction) is significantly smaller compared with the increase in Ser-845 phosphorylation seen in both the fraction of GluA1 not phosphorylated at Thr-840 (unbound fraction; *, $p < 0.05$) and total lysate before immunoprecipitation (input, **, $p < 0.01$). *C*, peptide competition assay comparing the ability of Ser-845-phosphorylated (*open circles*; $IC_{50} = 0.43 \pm 0.04$ ng/ml) and Ser-845/Thr-840-phosphorylated peptides (*filled circles*; $IC_{50} = 0.36 \pm 0.02$ ng/ml) to inhibit binding of phospho-Ser-845 antibody to Ser-845-phosphorylated GluA1 ($n = 4$ for each, Hill coefficients = 1.9 for both peptides). At the peptide concentrations tested a peptide phosphorylated at Thr-840 alone (*triangles*, $n = 3$) had no effect. *IB*, immunoblot.

Because of the close proximity of Thr-840 and Ser-845 in the C terminus of GluA1, another alternative explanation for the smaller increase in Ser-845 phosphorylation in Thr-840-phosphorylated GluA1 is that Thr-840 phosphorylation inhibits the ability of the phospho-Ser-845 antibody to recognize Ser-845-phosphorylated GluA1. Thus, as an additional control, we used a peptide competition assay to determine whether the ability of the anti-phospho-Ser-845 antibody to recognize Ser-845-phosphorylated GluA1 is reduced by GluA1 phosphorylation at Thr-840. As shown in Fig. 5*C*, the ability of this antibody to recognize Ser-845-phosphorylated GluA1 was blocked equally well by peptides phosphorylated at Ser-845 alone or at both Thr-840 and Ser-845. In contrast, a peptide-phosphorylated Thr-840 alone had no effect (Fig. 5*C*). This indicates that the ability of the phospho-Ser-845 antibody to recognize Ser-845-phosphorylated GluA1 is not altered by GluA1 phosphorylation at Thr-840.

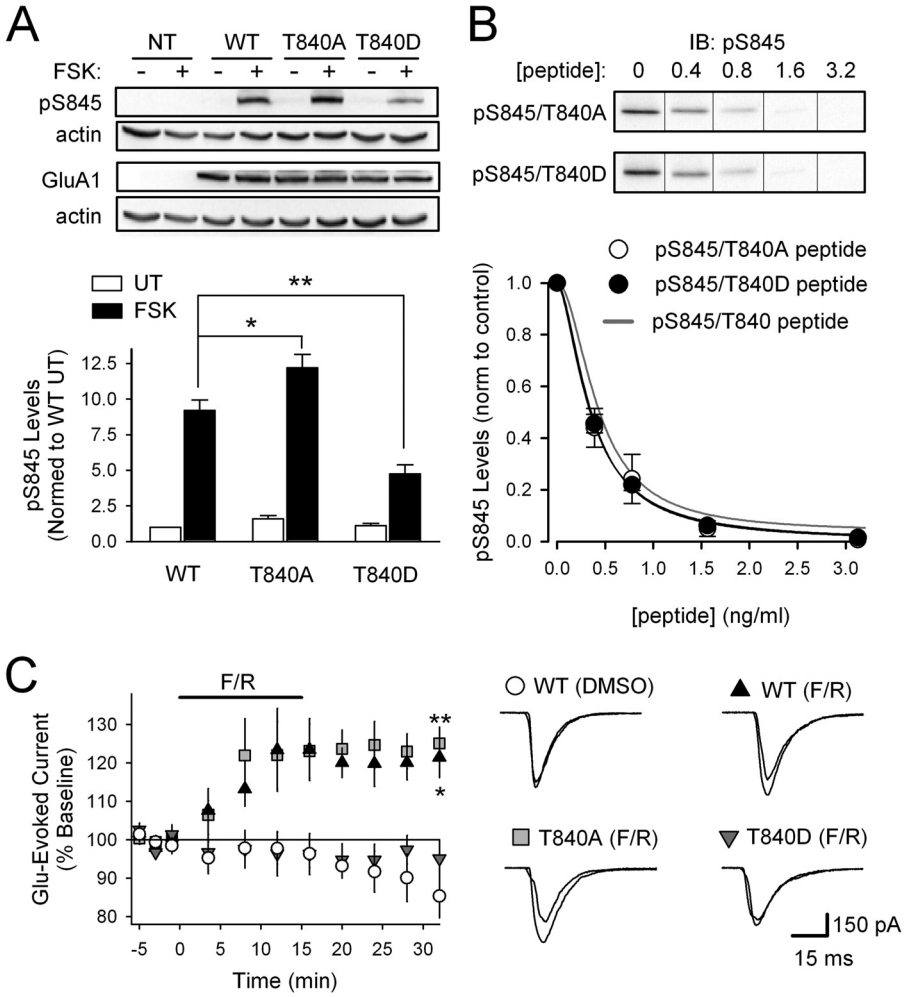

FIGURE 6. **Mimicking Thr-840 phosphorylation inhibits GluA1 phosphorylation at Ser-845.** *A*, compared with HEK-293 cells expressing WT full-length GluA1, increases in GluA1 Ser-845 phosphorylation induced by FSK (1 μM, 10 min) are significantly enhanced in cells expressing GluA1-T840A ($n = 6$; *, $p < 0.005$) and significantly reduced in cells expressing GluA1-T840D GluA1 ($n = 6$; **, $p < 0.005$). Mock transfected (*NT*) controls are also shown. *B*, phospho-Ser-845 (*pS845*) peptide competition assays testing effects of alanine (*open symbols*, $IC_{50} = 0.39 \pm 0.01$ ng/ml, $n = 5$) or aspartate (*filled symbols*, $IC_{50} = 0.35 \pm 0.03$ ng/ml, $n = 4$) substitutions for Thr-840 on antibody recognition of Ser-845 phosphorylated GluA1. The *gray line* corresponds to results from competition assays using phospho-Ser-845 peptide shown in Fig. 5*C*. *IB*, immunoblot. *C*, PKA activation (bath application of 50 μM FSK, 0.1 μM rolilpram (*F/R*), indicated by the *bar*) significantly enhances glutamate-evoked currents in HEK-293 cells expressing GluA1-WT ($n = 5$; *, $p < 0.05$ compared with base line for all points after 10 min of FSK) or GluA1-T840A ($n = 6$; **, $p < 0.01$ compared with base line for all points after 10 min of FSK) but had no effect in cells expressing GluA1-T840D ($n = 6$). Vehicle control experiments (0.11% DMSO, GluA1-WT, $n = 4$) are shown for comparison. Traces show example currents evoked during base line and 15 min after FSK/rolilpram application.

As a second test of the ability of Thr-840 phosphorylation to inhibit Ser-845 phosphorylation, we next examined whether increases in GluA1 Ser-845 phosphorylation induced by activating PKA with the adenylyl cyclase activator FSK were inhibited in HEK-293 cells expressing a Thr-840 phosphomimetic form of GluA1 where an aspartate replaced threonine at position 840 (GluA1-T840D) (Fig. 6*A*). FSK-induced increases in Ser-845 phosphorylation were strongly inhibited in cells expressing GluA1-T840D compared with cells expressing wild type GluA1 (GluA1-WT) ($p < 0.001$). Moreover, FSK-induced Ser-845 phosphorylation was significantly enhanced in cells expressing a mutant form of GluA1 where Thr-840 was replaced by a nonphosphorylate-able alanine (GluA1-T840A) ($p < 0.005$), suggesting that preventing phosphorylation of Thr-840 by endogenous kinases facilitates PKA phosphorylation of Ser-845 (Fig. 6*A*). To examine whether the amino acid substitutions used in these experiments might alter the ability of the phospho-Ser-845 antibody to recognize Ser-845-phosphorylated GluA1, we performed peptide competition assays with Ser-845-phosphorylated peptides containing either an aspartate or alanine at position 840. As shown in Fig. 6*B*, neither amino acid substitution altered the ability of Ser-845-phosphorylated peptides to inhibit antibody recognition of Ser-845-phosphorylated GluA1.

As a final test of the ability of Thr-840 phosphorylation to inhibit GluA1 phosphorylation at Ser-845, we took advantage of previous results demonstrating that Ser-845 phosphorylation mediates PKA-induced increases in AMPAR surface expression (24) and channel activity (39, 40) in HEK-293 cells expressing GluA1. Thus, we examined PKA modulation of glutamate-evoked currents in GluA1-transfected HEK-293 cells expressing GluA1-WT, GluA1-T840A, or GluA1-T840D forms of GluA1. Application of glutamate (10 mM, 100 ms) induced similar currents in HEK-293 cells expressing these different

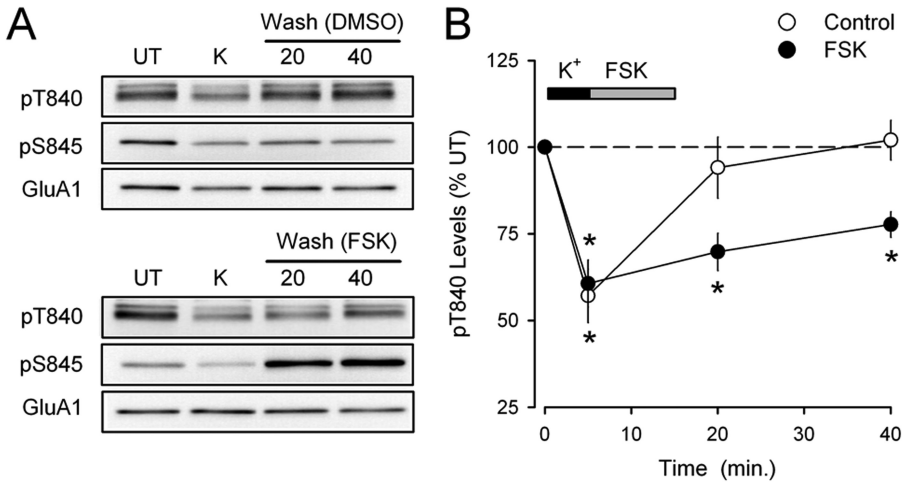

FIGURE 7. **GluA1 Ser-845 phosphorylation inhibits Thr-840 phosphorylation *in vivo*.** *A*, immunoblots showing the effects of bath application of FSK (50 μM, 10 min) or 0.1% DMSO (vehicle control) for 10 min during high-K^+ (*K*) ACSF washout on GluA1 Thr-840 (*pT840*) and Ser-845 (*pS845*) phosphorylation. Note the robust increase in Ser-845 phosphorylation induced by FSK. *UT*, untreated. *B*, although Thr-840 rapidly re-phosphorylates in vehicle control experiments ($n = 4$), Thr-840 re-phosphorylation is significantly inhibited when PKA is activated with FSK during high-K^+ ACSF washout ($n = 4$; *, $p < 0.05$ compared with untreated control slices).

forms of GluA1, suggesting that Thr-840 phosphorylation has little, if any, effect on basal AMPAR activity (data not shown). As shown in Fig. 6*C*, activating PKA with a 15-min bath application of 50 μM FSK and the phosphodiesterase inhibitor rolipram (0.1 μM) significantly potentiated glutamate-evoked currents in cells expressing GluA1-WT ($p < 0.05$, $n = 5$) or GluA1-T840A ($p < 0.01$, $n = 6$). In contrast, PKA activation had no effect on glutamate-evoked currents in cells expressing the Thr-840 phosphomimetic GluA1-T840D ($n = 6$) (Fig. 6*C*). Only a modest rundown in glutamate-evoked currents was seen in vehicle control experiments (0.11% DMSO) using cells expressing GluA1-WT (Fig. 6*C*). Thus, consistent with the presence of inhibitory interactions between Thr-840 and Ser-845, mimicking GluA1 phosphorylation at Thr-840 inhibits phospho-Ser-845 dependent modulation of AMPAR function.

GluA1 Phosphorylation at Ser-845 Inhibits Thr-840 Phosphorylation—Given the inhibitory influence Thr-840 phosphorylation exerts over GluA1 phosphorylation at Ser-845, we next asked whether Ser-845 phosphorylation can similarly regulate Thr-840 phosphorylation. We first investigated this question by examining whether increasing GluA1 Ser-845 phosphorylation could inhibit the rapid re-phosphorylation of Thr-840 that occurs after high-K^+-induced dephosphorylation. For these experiments we used a protocol similar to that shown in Fig. 1*B* where hippocampal slices from the same animal were either untreated or exposed to a 5-min application of high-K^+ ACSF and collected either immediately after depolarization or at different times after high-K^+ ACSF washout (15 and 35 min). In control experiments ACSF containing 0.1% DMSO was applied during the first 10 min of high-K^+ washout, and as expected, GluA1 Thr-840 phosphorylation returned to basal levels seen in untreated control slices within 15 min post-depolarization (Fig. 7, *A* and *B*). In contrast, application of ACSF containing 50 μM FSK during the first 10 min of high-K^+ washout increased Ser-845 phosphorylation and significantly inhibited Thr-840 re-phosphorylation (Fig. 7, *A* and *B*).

As a more direct test of the ability of Ser-845 phosphorylation to inhibit GluA1 phosphorylation at Thr-840, we next examined the ability of purified protein kinases to phosphorylate Thr-840 on either WT or Ser-845 phosphomimetic (S845D) C-terminal GluA1-GST fusion proteins. Consistent with the notion that Ser-845 phosphorylation can inhibit GluA1 phosphorylation at Thr-840, mimicking phosphorylation at Ser-845 strongly inhibited PKC phosphorylation of Thr-840 (Fig. 8*A*). Substitution of an aspartate for Ser-845 only slightly reduced the ability of Thr-840-phosphorylated peptides to block the ability of the phospho-Thr-840 antibody to recognize Thr-840-phosphorylated GluA1 (Fig. 8*C*). Thus, it seems unlikely that the pronounced decrease in PKC phosphorylation of GluA1(S845D)-GST fusion protein reflects a disruption of the phospho-Thr-840 antibody to recognize Thr-840 phosphorylation in the GluA1-S845D fusion protein. Indeed, substitution of an aspartate for Ser-845 had no effect on CaMKII phosphorylation of Thr-840 (Fig. 8, *A* and *B*). In addition to providing evidence for bidirectional, inhibitory interactions between Thr-840 and Ser-845, these results suggest that Ser-845 phosphorylation may act as a conditional switch that determines the upstream signaling pathways regulating Thr-840 phosphorylation. In addition, mimicking phosphorylation at Ser-845 had no effect on PKC and CaMKII phosphorylation of GluA1 at Ser-831 ($n = 4$ for both kinases, data not shown). This indicates that the ability of Ser-845 phosphorylation to inhibit phosphorylation of other sites in the C terminus of GluA1 is spatially restricted to nearby phosphorylation sites.

DISCUSSION

Although neuronal depolarization induces a Ca^{2+}-dependent dephosphorylation of AMPAR GluA1 subunits at both Thr-840 and Ser-845, our results indicate that distinct Ca^{2+}-dependent signaling pathways regulate GluA1 phosphorylation at these sites. The highly specific role for NMDAR-mediated increases in Ca^{2+} in Ser-845 dephosphorylation and activation of VGCCs in triggering GluA1 Thr-840 dephosphorylation is particularly interesting and may provide a mechanism for producing distinct patterns of GluA1 phosphorylation in response to different patterns of neuronal activity. For example, although

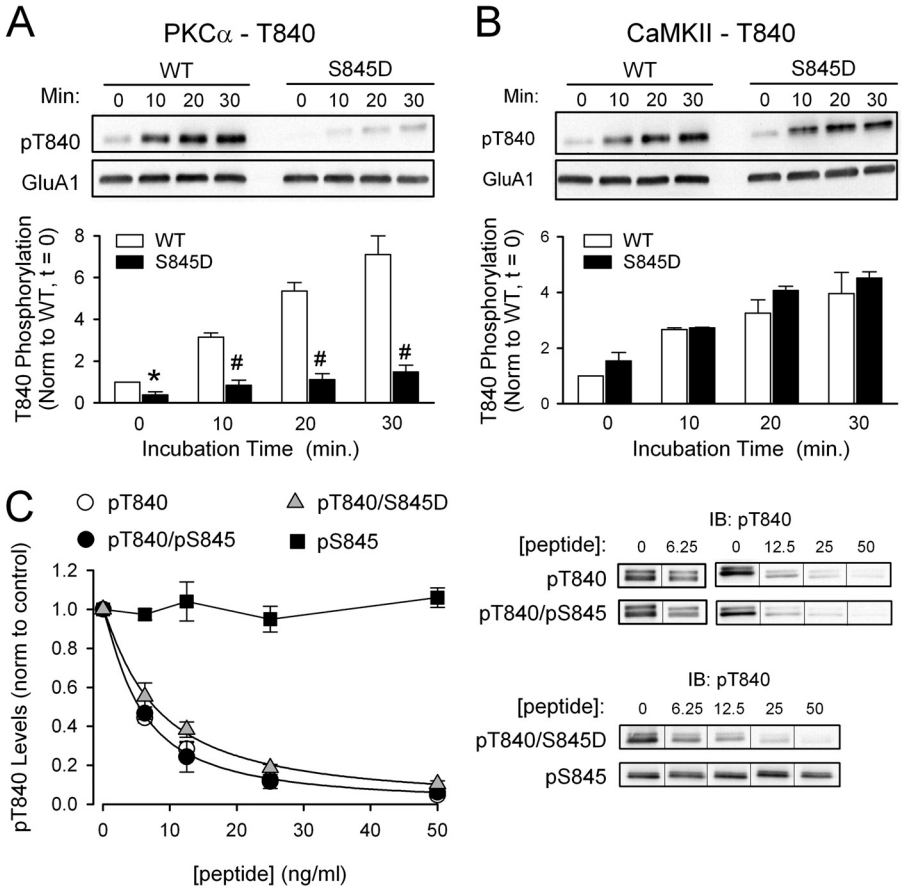

FIGURE 8. **GluA1 Ser-845 phosphorylation inhibits Thr-840 phosphorylation *in vitro*.** *A* and *B*, WT and Ser-845 phospho-mimic (*S845D*) versions of the C-terminal GluA1-GST fusion protein were incubated with purified PKC (*A*) or CaMKII (*B*) and immunoblotting with phospho-specific antibodies was used to measure Thr-840 phosphorylation (*pT840*). Mimicking Ser-845 phosphorylation inhibited Thr-840 phosphorylation by PKC ($n = 4$; #, $p < 0.005$ compared with WT GluA1-GST fusion protein) but had no effect on CaMKII phosphorylation of Thr-840 ($n = 4$). *C*, phosphopeptide competition assays testing the effects of Ser-845 phosphorylation (*filled circles*, $IC_{50} = 5.4$ ng/ml, $n = 4$) or substitution of aspartate for Ser-845 (*triangles*, $IC_{50} = 7.7$ ng/ml, $n = 4$) on the ability of a Thr-840-phosphorylated peptide (*open circles*, $IC_{50} = 5.4$ ng/ml, $n = 6$) to inhibit phospho-Thr-840 antibody recognition of Thr-840-phosphorylated GluA1. At the concentrations tested a peptide phosphorylated only at Ser-845 (*pS845*) had no effect (*squares*, $n = 3$). *IB*, immunoblot.

activation of NMDARs and VGCCs during coincident pre- and postsynaptic activity could trigger GluA1 dephosphorylation at both Ser-845 and Thr-840, postsynaptic activity alone will selectively dephosphorylate GluA1 at Thr-840. The pattern of Thr-840 and Ser-845 phosphorylation could thus provide a mechanism for encoding information about the recent history of pre- and/or postsynaptic activity within the C terminus of GluA1 subunits. Future experiments comparing the effects of dual Thr-840/Ser-845 phosphorylation *versus* monophosphorylation at either site on AMPAR function and trafficking could provide important information regarding how this potential "phospho-code" might be used to modulate excitatory synaptic transmission. In this context it is interesting that although Ser-845 dephosphorylation is required for LTD (22), experimental manipulations that induce a persistent decrease in Ser-845 phosphorylation and a transient decrease in Thr-840 phosphorylation (high-K^+ ACSF, NMDA application in normal ACSF) have no lasting effect on synaptic strength. This suggests that although Ser-845 dephosphorylation may be necessary for LTD, it is not sufficient. Interestingly, a recent study found that the conductance of AMPAR ion channels is enhanced by Thr-840 phosphorylation (28), and we find that LTD induced by pharmacological activation of NMDA receptors is associated with a persistent decrease in GluA1 phosphorylation at Thr-840 (Fig. 1). Together these results suggest that Thr-840 dephosphorylation may contribute to the weakening of synaptic strength in LTD.

Although blocking VGCC with Co^{2+} prevented depolarization-induced dephosphorylation of Thr-840, Co^{2+} ions inhibit a number of different types of VGCCs, and thus our results provide little insight into the role of a specific VGCC(s). One possibility is that Co^{2+} prevents Thr-840 dephosphorylation by inhibiting presynaptic VGCCs and blocking the release of neurotransmitters that activate protein phosphatases via postsynaptic G protein-coupled receptors. However, depleting intracellular Ca^{2+} stores with thapsigargin had no effect on depolarization-induced Thr-840 dephosphorylation. This indicates that activation of G protein-coupled receptors that trigger Ca^{2+} release from intracellular stores is not involved. Moreover, although B56δ subunit-containing forms of PP2A can be phosphorylated and activated by PKA or PKC (45, 46), activation of these protein kinases has no effect on basal levels of GluA1 phosphorylation at Thr-840 (25, 26). It thus seems unlikely that Co^{2+} blocks depolarization-induced Thr-840 dephosphorylation by inhibiting presynaptic VGCCs and preventing the activation of postsynaptic G protein-coupled recep-

tors that activate PP2A via these protein kinases. A second possibility is that inhibition of postsynaptic VGCCs underlies the Co^{2+} block of depolarization-induced Thr-840 dephosphorylation. If so, our results suggest that Ca^{2+} signaling within highly restricted domains near NMDARs and VGCCs in dendritic spines and dendrites has a crucial role in regulating GluA1 phosphorylation at Ser-845 and Thr-840. Although the notion that signaling dependent on Ca^{2+} micro/nanodomains in structures as spatially restricted as dendritic spines is surprising, it is not without precedent (47). For example, SK type Ca^{2+}-activated K^+ channels in dendritic spines are selectively activated by Ca^{2+} influx via $CaV_{2.3}$ type VGCCs (R-type) (48) despite the fact that increases in dendritic spine Ca^{2+} during synaptic activity are predominately mediated by NMDARs (48–50). One possibility consistent with our findings is that selective activation of PP2B by NMDAR-mediated increases in intracellular Ca^{2+} mediates dephosphorylation of GluA1 at Ser-845, whereas Thr-840 is dephosphorylated by Ca^{2+}-sensitive, PR72 subunit-containing forms of PP2A (51) coupled to VGCCs. Future studies focused on identifying the particular VGCC(s) involved, the role of PP2A, and the protein interactions responsible for coupling VGCC activation to signaling pathways that selectively lead to dephosphorylation of GluA1 Thr-840 will be informative.

Common phosphorylation signaling motifs such as kinase divergence, where a single protein kinase phosphorylates multiple target sites, and kinase convergence, where a single site is phosphorylated by multiple protein kinases, are found within the C terminus of AMPAR GluA1 subunits (2, 32). In addition to these intermolecular signaling motifs, our results suggest that the close proximity of Thr-840 and Ser-845 gives rise to an intramolecular phosphorylation signaling motif in GluA1 where phosphorylation of one site interferes with phosphorylation of the other.

The inhibitory interactions between Thr-840 and Ser-845 may give rise to state-dependent, conditional signaling that can act in a switch-like fashion to regulate the ability of some upstream signaling pathways to modify AMPAR function. In addition, because Thr-840 and Ser-845 are dephosphorylated in response to increases in intracellular Ca^{2+} arising from distinct channels, the resetting of these switches by dephosphorylation will be controlled by distinct patterns of neuronal activity. Together, the unique modulation of Thr-840 and Ser-845 and the interactions between these sites may provide a molecular mechanism underlying state-dependent forms of metaplasticity (52, 53). For example, high-frequency synaptic stimulation induced phosphorylation of GluA1 at Ser-845 is highly dependent on synaptic state and only occurs at synapses that have previously undergone LTD (21). Previous findings suggesting that basal levels of GluA1 Thr-840 phosphorylation are relatively high (26) and our observations that Thr-840 phosphorylation inhibits PKA phosphorylation of Ser-845 (Fig. 5) and that Thr-840 is persistently dephosphorylated during LTD (Fig. 1) (25) provide a mechanistic basis for this phenomenon. Clearly, a complete understanding of the role of Thr-840/Ser-845 interactions in synaptic plasticity, metaplasticity, and AMPAR function will require additional study. Our results suggest, however, that because of these interactions, the C terminus of AMPAR GluA1 subunits is not only a target of the protein kinase and protein phosphatase signaling pathways underlying LTP and LTD but can also serve as a signal integration platform for these signaling pathways that may be capable of surprisingly sophisticated information processing.

Acknowledgments—We are grateful to Drs. Seth Grant, Marcelo Coba, and Walter Babiec for helpful comments during the course of this work. The GluA1 C terminus GST fusion protein (plasmid pGEX-4T-3 GluR1CT) was kindly provided by T. Soderling (Oregon Health Sciences University).

REFERENCES

1. Derkach, V. A., Oh, M. C., Guire, E. S., and Soderling, T. R. (2007) Regulatory mechanisms of AMPA receptors in synaptic plasticity. *Nat. Rev. Neurosci.* **8,** 101–113
2. Santos, S. D., Carvalho, A. L., Caldeira, M. V., and Duarte, C. B. (2009) Regulation of AMPA receptors and synaptic plasticity. *Neuroscience* **158,** 105–125
3. Lee, H. K. (2006) Synaptic plasticity and phosphorylation. *Pharmacol. Ther.* **112,** 810–832
4. Boehm, J., Kang, M. G., Johnson, R. C., Esteban, J., Huganir, R. L., and Malinow, R. (2006) Synaptic incorporation of AMPA receptors during LTP is controlled by a PKC phosphorylation site on GluR1. *Neuron* **51,** 213–225
5. Mammen, A. L., Kameyama, K., Roche, K. W., and Huganir, R. L. (1997) Phosphorylation of the α-amino-3-hydroxy-5-methylisoxazole4-propionic acid receptor GluR1 subunit by calcium/calmodulin-dependent kinase II. *J. Biol. Chem.* **272,** 32528–32533
6. Barria, A., Derkach, V., and Soderling, T. (1997) Identification of the Ca^{2+}/calmodulin-dependent protein kinase II regulatory phosphorylation site in the α-amino-3-hydroxyl-5-methyl-4-isoxazole-propionate-type glutamate receptor. *J. Biol. Chem.* **272,** 32727–32730
7. Barria, A., Muller, D., Derkach, V., Griffith, L. C., and Soderling, T. R. (1997) Regulatory phosphorylation of AMPA-type glutamate receptors by CaM-KII during long-term potentiation. *Science* **276,** 2042–2045
8. Benke, T. A., Lüthi, A., Isaac, J. T., and Collingridge, G. L. (1998) Modulation of AMPA receptor unitary conductance by synaptic activity. *Nature* **393,** 793–797
9. Derkach, V., Barria, A., and Soderling, T. R. (1999) Ca^{2+}/calmodulin-kinase II enhances channel conductance of α-amino-3-hydroxy-5-methyl-4-isoxazolepropionate type glutamate receptors. *Proc. Natl. Acad. Sci. U.S.A.* **96,** 3269–3274
10. Poncer, J. C., Esteban, J. A., and Malinow, R. (2002) Multiple mechanisms for the potentiation of AMPA receptor-mediated transmission by α-Ca^{2+}/calmodulin-dependent protein kinase II. *J. Neurosci.* **22,** 4406–4411
11. Lüthi, A., Wikström, M. A., Palmer, M. J., Matthews, P., Benke, T. A., Isaac, J. T., and Collingridge, G. L. (2004) Bidirectional modulation of AMPA receptor unitary conductance by synaptic activity. *BMC Neurosci.* **5,** 44
12. Palmer, M.J., Isaac, J.T., Collingridge, G.L. (2004) Multiple, developmentally regulated expression mechanisms of long-term potentiation at CA1 synapses. *J. Neurosci.* **24,** 4903–4911
13. Kristensen, A. S., Jenkins, M. A., Banke, T. G., Schousboe, A., Makino, Y., Johnson, R. C., Huganir, R., and Traynelis, S. F. (2011) Mechanism of Ca^{2+}/calmodulin-dependent kinase II regulation of AMPA receptor gating. *Nat. Neurosci.* **14,** 727–735
14. Esteban, J. A., Shi, S. H., Wilson, C., Nuriya, M., Huganir, R. L., and Malinow, R. (2003) PKA phosphorylation of AMPA receptor subunits controls synaptic trafficking underlying plasticity. *Nat. Neurosci.* **6,** 136–143
15. Oh, M. C., Derkach, V. A., Guire, E. S., and Soderling, T. R. (2006) Extrasynaptic membrane trafficking regulated by GluR1 serine 845 phosphorylation primes AMPA receptors for long-term potentiation. *J. Biol. Chem.* **281,** 752–758
16. Hu, H., Real, E., Takamiya, K., Kang, M. G., Ledoux, J., Huganir, R. L., and

Malinow, R. (2007) Emotion enhances learning via norepinephrine regulation of AMPA-receptor trafficking. *Cell* **131,** 160–173
17. Seol, G. H., Ziburkus, J., Huang, S., Song, L., Kim, I. T., Takamiya, K., Huganir, R. L., Lee, H. K., and Kirkwood, A. (2007) Neuromodulators control the polarity of spike-timing-dependent synaptic plasticity. *Neuron* **55,** 919–929
18. Tenorio, G., Connor, S. A., Guévremont, D., Abraham, W. C., Williams, J., O'Dell, T. J., and Nguyen, P. V. (2010) "Silent" priming of translation-dependent LTP by β-adrenergic receptors involves phosphorylation and recruitment of AMPA receptors. *Learn. Mem.* **17,** 627–638
19. Kameyama, K., Lee, H. K., Bear, M. F., and Huganir, R. L. (1998) Involvement of a postsynaptic protein kinase A substrate in the expression of homosynaptic long-term depression. *Neuron* **21,** 1163–1175
20. Lee, H. K., Kameyama, K., Huganir, R. L., and Bear, M. F. (1998) NMDA induces long-term synaptic depression and dephosphorylation of the GluR1 subunit of AMPA receptors in hippocampus. *Neuron* **21,** 1151–1162
21. Lee, H. K., Barbarosie, M., Kameyama, K., Bear, M. F., and Huganir, R. L. (2000) Regulation of distinct AMPA receptor phosphorylation sites during bidirectional synaptic plasticity. *Nature* **405,** 955–959
22. Lee, H. K., Takamiya, K., He, K., Song, L., and Huganir, R. L. (2010) Specific roles of AMPA receptor subunit GluR1 (GluA1) phosphorylation sites in regulating synaptic plasticity in the CA1 region of hippocampus. *J. Neurophysiol.* **103,** 479–489
23. Ehlers, M. D. (2000) Reinsertion or degradation of AMPA receptors determined by activity-dependent endocytic sorting. *Neuron* **28,** 511–525
24. Man, H. Y., Sekine-Aizawa, Y., and Huganir, R. L. (2007) Regulation of {α}-amino-3-hydroxy-5-methyl-4-isoxazolepropionic acid receptor trafficking through PKA phosphorylation of the Glu receptor 1 subunit. *Proc. Natl. Acad. Sci. U.S.A.* **104,** 3579–3584
25. Delgado, J. Y., Coba, M., Anderson, C. N., Thompson, K. R., Gray, E. E., Heusner, C. L., Martin, K. C., Grant, S. G., and O'Dell, T. J. (2007) NMDA receptor activation dephosphorylates AMPA receptor glutamate receptor 1 subunits at threonine 840. *J. Neurosci.* **27,** 13210–13221
26. Lee, H. K., Takamiya, K., Kameyama, K., He, K., Yu, S., Rossetti, L., Wilen, D., and Huganir, R. L. (2007) Identification and characterization of a novel phosphorylation site on the GluR1 subunit of AMPA receptors. *Mol. Cell. Neurosci.* **36,** 86–94
27. Munton, R. P., Tweedie-Cullen, R., Livingstone-Zatchej, M., Weinandy, F., Waidelich, M., Longo, D., Gehrig, P., Potthast, F., Rutishauser, D., Gerrits, B., Panse, C., Schlapbach, R., and Mansuy, I. M. (2007) Qualitative and quantitative analyses of protein phosphorylation in naive and stimulated mouse synaptosomal preparations. *Mol. Cell Proteomics* **6,** 283–293
28. Jenkins, M. A., Wells, G., Bachman, J., Snyder, J. P., Jenkins, A., Huganir, R. L., Oswald, R. E., and Traynelis, S. F. (2014) Regulation of GluA1 α-amino-3-hydroxy-5-methyl-4-isoxazole propionic acid receptor function by protein kinase C at serine 818 and threonine 840. *Mol. Pharmacol.* **85,** 618–629
29. Roach, P. J. (1991) Multisite and hierarchal protein phosphorylation. *J. Biol. Chem.* **266,** 14139–14142
30. Kemp, B. E., and Pearson, R. B. (1990) Protein kinase recognition sequence motifs. *Trends Biochem. Sci.* **15,** 342–346
31. Ubersax, J. A., and Ferrell, J. E., Jr. (2007) Mechanisms of specificity in protein phosphorylation. *Nat. Rev. Mol. Cell Biol.* **8,** 530–541
32. Coba, M. P., Pocklington, A. J., Collins, M. O., Kopanitsa, M. V., Uren, R. T., Swamy, S., Croning, M. D., Choudhary, J. S., and Grant, S. G. (2009) Neurotransmitters drive combinatorial multistate postsynaptic density networks. *Sci. Signal.* **2,** ra19
33. Collins, M. O., Yu, L., Coba, M. P., Husi, H., Campuzano, I., Blackstock, W. P., Choudhary, J. S., and Grant, S. G. (2005) Proteomic analysis of *in vivo* phosphorylated synaptic proteins. *J. Biol. Chem.* **280,** 5972–5982
34. Carlisle, H. J., Manzerra, P., Marcora, E., and Kennedy, M. B. (2008) SynGAP regulates steady-state and activity-dependent phosphorylation of cofilin. *J. Neurosci.* **28,** 13673–13683
35. Vanhoose, A. M., Clements, J. M., and Winder, D. G. (2006) Novel blockade of protein kinase A-mediated phosphorylation of AMPA receptors. *J. Neurosci.* **26,** 1138–1145
36. Vanhoose, A. M., and Winder, D. G. (2003) NMDA and β-adrenergic receptors differentially signal phosphorylation of glutamate receptor type 1 in area CA1 of hippocampus. *J. Neurosci.* **23,** 5827–5834
37. Honkanen, R. E. (1993) Cantharidin, another natural toxin that inhibits the activity of serine/threonine protein phosphatases types 1 and 2A. *FEBS Lett.* **330,** 283–286
38. Tokumitsu, H., Chijiwa, T., Hagiwara, M., Mizutani, A., Terasawa, M., and Hidaka, H. (1990) KN-62, 1-[*N*,*O*-bis(5-isoquinolinesulfonyl)-*N*-methyl-L-tyrosyl]-4-phenylpiperazine, a specific inhibitor of Ca^{2+}/calmodulin-dependent protein kinase II. *J. Biol. Chem.* **265,** 4315–4320
39. Roche, K. W., O'Brien, R. J., Mammen, A. L., Bernhardt, J., and Huganir, R. L. (1996) Characterization of multiple phosphorylation sites on the AMPA receptor GluR1 subunit. *Neuron* **16,** 1179–1188
40. Banke, T. G., Bowie, D., Lee, H., Huganir, R. L., Schousboe, A., and Traynelis, S. F. (2000) Control of GluR1 AMPA receptor function by cAMP-dependent protein kinase. *J. Neurosci.* **20,** 89–102
41. Pinna, L. A., and Ruzzene, M. (1996) How do protein kinases recognize their substrates? *Biochim. Biophys. Acta* **1314,** 191–225
42. Lu, W., Shi, Y., Jackson, A. C., Bjorgan, K., During, M. J., Sprengel, R., Seeburg, P. H., and Nicoll, R. A. (2009) Subunit composition of synaptic AMPA receptors revealed by a single-cell genetic approach. *Neuron* **62,** 254–268
43. Balasuriya, D., Goetze, T. A., Barrera, N. P., Stewart, A. P., Suzuki, Y., and Edwardson, J. M. (2013) α-Amino-3-hydroxy-5-methyl-4-isoxazole propionic acid (AMPA) and *N*-methyl-D-aspartate (NMDA) receptors adopt different subunit arrangements. *J. Biol. Chem.* **288,** 21987–21998
44. Mansour, M., Nagarajan, N., Nehring, R. B., Clements, J. D., and Rosenmund, C. (2001) Heteromeric AMPA receptors assemble with a preferred subunit stoichiometry and spatial arrangement. *Neuron* **32,** 841–853
45. Ahn, J. H., Kim, Y., Kim, H. S., Greengard, P., and Nairn, A. C. (2011) Protein kinase C-dependent dephosphorylation of tyrosine hydroxylase requires the B56δ heterotrimeric form of protein phosphatase 2A. *PLoS ONE* **6,** e26292
46. Ahn, J. H., McAvoy, T., Rakhilin, S. V., Nishi, A., Greengard, P., and Nairn, A. C. (2007) Protein kinase A activates protein phosphatase 2A by phosphorylation of the B56δ subunit. *Proc. Natl. Acad. Sci. U.S.A.* **104,** 2979–2984
47. Bloodgood, B. L., and Sabatini, B. L. (2007) Ca^{2+} signaling in dendritic spines. *Curr. Opin. Neurobiol.* **17,** 345–351
48. Bloodgood, B. L., and Sabatini, B. L. (2007) Nonlinear regulation of unitary synaptic signals by CaV(2.3) voltage-sensitive calcium channels located in dendritic spines. *Neuron* **53,** 249–260
49. Yuste, R., Majewska, A., Cash, S. S., and Denk, W. (1999) Mechanisms of calcium influx into hippocampal spines: heterogeneity among spines, coincidence detection by NMDA receptors, and optical quantal analysis. *J. Neurosci.* **19,** 1976–1987
50. Kovalchuk, Y., Eilers, J., Lisman, J., and Konnerth, A. (2000) NMDA receptor-mediated subthreshold Ca^{2+} signals in spines of hippocampal neurons. *J. Neurosci.* **20,** 1791–1799
51. Ahn, J. H., Sung, J. Y., McAvoy, T., Nishi, A., Janssens, V., Goris, J., Greengard, P., and Nairn, A. C. (2007) The B″/PR72 subunit mediates Ca^{2+}-dependent dephosphorylation of DARPP-32 by protein phosphatase 2A. *Proc. Natl. Acad. Sci. U.S.A.* **104,** 9876–9881
52. Montgomery, J. M., and Madison, D. V. (2004) Discrete synaptic states define a major mechanism of synapse plasticity. *Trends Neurosci.* **27,** 744–750
53. Abraham, W. C. (2008) Metaplasticity: tuning synapses and networks for plasticity. *Nat. Rev. Neurosci.* **9,** 387